Thin Solid Films 665 (2018) 159–163

Contents lists available at ScienceDirect

Thin Solid Films

journal homepage: www.elsevier.com/locate/tsf

Low temperature incorporation of selenium in Cu_2ZnSnS_4: Diffusion and nucleation

Sigbjørn Grini[a,*], Nils Ross[a,b], Clas Persson[a], Charlotte Platzer-Björkman[b], Lasse Vines[a]

[a] Department of Physics, Center for Materials Science and Nanotechnology, University of Oslo, P.O.Box 1048, Blindern, N-0316 Oslo, Norway
[b] Ångström Solar Center, Division of Solid State Electronics, Uppsala University, Uppsala, Uppland 75120, Sweden

ARTICLE INFO

Keywords:
Cu2ZnSnS4
Selenium diffusion
Band gap grading
Nucleation
Recrystallization
Grain boundary diffusion
Diffusion
Secondary ion mass spectrometry

ABSTRACT

Band gap grading of $Cu_2ZnSn(S,Se)_4$ (CZTSSe) solar cells can be achieved by varying the S_r = [S]/([S] + [Se]) ratio in the absorber layer with depth. One approach is a two-step annealing process where the absorber is first sulfurized to Cu_2ZnSnS_4 (CZTS) followed by selenization to form CZTSSe. However, once nucleation of CZTSSe initiates, the rapid interchange of S and Se limits the control over the S_r ratio with depth. Here, we have studied incorporation of Se into CZTS and observed the behavior of Se below and up to the nucleation temperature of CZTSSe. Se diffusion at 337 and 360 °C is dominated by grain boundary diffusion while some increase of Se is also seen in the region from 100 to 800 nm from the surface. After selenization at 409 °C, recrystallization is observed and CZTSSe grains are formed. The recrystallization is more rapid for a smaller average grain size and is facilitated by diffusion of Na from the back contact. The grain boundary diffusion is identified with secondary ion mass spectrometry measurements by measuring the accumulation in the CZTS/Mo interface for three samples with different average grain size.

1. Introduction

The best $Cu_2ZnSn(S,Se)_4$ (CZTSSe) devices produced to date have introduced the chalcogens S and Se either as part of the precursor or as gas during the crystallization process [1–5]. By including both chalcogens in the complex crystallization process, control of their diffusion and nucleation is limited, and it is difficult to obtain a controlled S_r = [S]/([S] + [Se]) ratio with depth. Nevertheless, there are pathways to achieve an S_r gradient in the CZTSSe layer by having S and Se annealed in two steps or through non-symmetric annealing conditions [2,6–8]. If the anneals are performed at low crystallization temperatures, partial recrystallization of the absorber may occur which results in a lateral non-homogeneous distribution of S and Se [9], which can falsely be interpreted as an S_r gradient with grazing incident X-ray diffraction (GIXRD) or conventional secondary ion mass spectrometry (SIMS) depth profile [10]. Previously, we have discussed the practical limitations of chalcogen control in the crystallization process, where sodium assists grain growth [11]. To achieve a controlled S_r gradient a possible approach is to complete a full crystallization with either S or Se and subsequently diffuse in the other chalcogen without triggering nucleation. The challenge is that the energy required to diffuse Se into the existing grains is similar or perhaps higher than the energy required to start to nuclear new grains. In this work we evaluate the diffusion of Se into CZTS at temperatures up to nucleation by annealing in a selenium ambient at 337, 360 and 409 °C for three samples with different average grain size.

2. Experimental details

Bilayer molybdenum back contact was sputtered onto a soda-lime glass substrate. Cu_2ZnSnS_4 precursors were co-sputtered using CuS, ZnS and SnS targets in a Lesker CMS-18 sputter system. Elemental compositions in the precursors were determined with Rutherford backscattering calibrated X-ray fluorescence (XRF) measurements. The samples were sulfurized into Cu_2ZnSnS_4 for 10, 20 and 40 min at 500 ± 10 °C in a tube furnace within a pyrolytic carbon coated graphite box with 80 mg of elemental sulfur placed in a small hole on each side of the box and an argon pressure in the furnace of 35 kPa. The temperature was chosen to avoid secondary phase formation and loss of sulfur as have previously shown to occur at higher temperatures for our furnace [12]. After sulfurization and initial characterization, each sample was subjected to an anneal in the same tube furnace with 90 mg Se in the graphite box and an argon pressure of 35 kPa at 337 ± 10, 360 ± 10 and 409 ± 10 °C for 30 min, from now on called “selenization”. The cation ratios and sulfurization conditions are described in Table 1.

---

[*] Corresponding author.
E-mail address: sigbjorn.grini@smn.uio.no (S. Grini).

https://doi.org/10.1016/j.tsf.2018.09.024
Received 15 June 2018; Received in revised form 10 August 2018; Accepted 12 September 2018

Table 1
Cation ratios measured with X-ray fluorescence of the precursor and sulfurization conditions in the tube furnace.

Sample name	Cation ratios		Sulfurization conditions	
	[Cu]/[Sn]	[Zn]/([Cu] + [Sn])	Temperature (°C)	Time (minutes)
A	1.92 ± 0.02	0.35 ± 0.02	500 ± 10	10
B	1.92 ± 0.02	0.35 ± 0.02	500 ± 10	20
C	1.92 ± 0.02	0.35 ± 0.02	500 ± 10	40

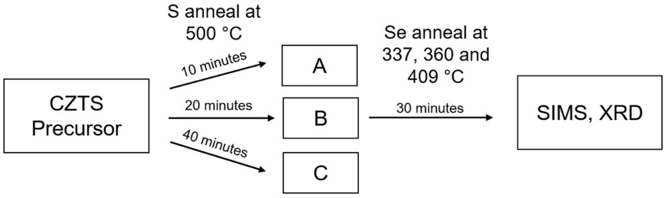

Fig. 1. Overview over the experiment. CZTS precursors were sulfurized at 500 °C for 10, 20 and 40 min and produced samples A, B and C respectively. Each sample was subsequently selenized at 337, 360 and 409 °C and characterized with secondary ion mass spectrometry (SIMS) and X-ray diffraction (XRD).

A Bruker AXS D8 Discover X-ray diffraction (XRD) system was used to study structural properties of the samples before and after selenization. Each sample was surveyed with a θ/2θ scan ranging from 10° to 65° with an increment of 0.01° and a high-resolution scan from 27° to 29° with an increment of 0.002° to study the (112) reflection in detail. Cross-sectional scanning electron microscopy (SEM) images were obtained using a Zeiss Leo 1550 with a 5 kV accelerating voltage. Top-view SEM images were obtained with JEOL JSM-IT300 with a 5 kV accelerating voltage. The samples were studied with secondary ion mass spectrometry (SIMS) using a Cameca IMS 7f magnetic sector instrument. 5 keV Cs^+ primary ions were mainly used, and the beam was rastered over an area of 150 × 150 μm^2 with a current of 20 nA. Secondary MCs^+ cluster ions were detected from the central part of the crater (33 μm in diameter), where “M” is the element of interest. The ionization of MCs^+ cluster ions is suggested to be less influenced by a change in concentration of matrix elements compared to that of M^+ ions since the Cs^+ ions are previously ionized as the primary beam [13]. The cluster $^{80}Se\ ^{133}Cs$ was considered most suited to observe Se given its abundance and $^{23}Na^{133}Cs$ was used to track Na. Control measurements were also carried out on selected samples by detecting negative ions with a 15 keV Cs^+ primary beam and positive ions with 10 keV $O_2{}^+$ primary beam to confirm that no significant interference occurred. The sputter time was converted to depth by measuring the depth of the crater with a Stylus profilometer. For measurements on the same sample after heat treatment the depth was calibrated with the inflection point of the $^{98}Mo^{133}Cs$ signal at the interface between CZTS and Mo. An overview over the experiment is displayed in Fig. 1.

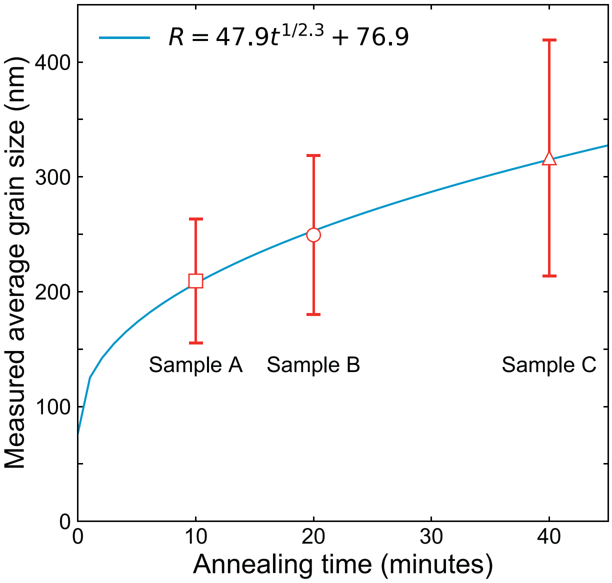

Fig. 3. Extracted average grain size, *R*, (red markers) and the variation (red bars), as a function of annealing temperature for the samples A, B and C which was sulfurized at 500 °C for 10, 20 and 40 min respectively from the same precursor. *R* was estimated using top view SEM images (not shown). 5 horizontal and 5 vertical equally spaced lines were drawn for two images for each sample. The blue line illustrates fitting equation for $R \propto t^{1/2.3}$, adapted from Ren et al. [12], and the parameters are shown in the legend. (For interpretation of the references to colour in this figure legend, the reader is referred to the web version of this article.)

3. Results and discussion

Fig. 2 displays cross sectional SEM images of the samples A, B and C which was sulfurized at 10, 20 and 40 min at 500 °C, respectively. The images show a ~1 μm CZTS layer on top of a Mo back contact, in addition to secondary phase formation of SnS_2 (in sample B). However, the amount of secondary phase formation was sufficiently low, so that it did not interfere with subsequent measurements. The variation in sulfurization time results in different average grain sizes as previously demonstrated with the same furnace and sputtering system, and where the average grain size, *R*, is dependent on annealing time, *t*, with $R \propto t^{1/n}$ where *n* is between 2.2 and 2.4 [12]. The average grain size was estimated by counting the number of grain boundaries over a line drawn across the image and divided by its length, as shown in Fig. 3, where the extracted average and variation in grain size, in addition to the estimate with $R \propto t^{1/2.3}$, are displayed. Indeed, Fig. 3 demonstrates that the average grain size increases with approximately 50% from the sample annealed for 10 min compared to that annealed for 40 min. Thus, one can expect that the influence of grain boundary diffusion is different for different sulfurization times.

Fig. 4 shows the $^{80}Se^{133}Cs$ signals measured with SIMS for sample B after selenizations at 337, 360 and 409 °C for 30 min. Similar temperature dependencies are observed for samples A and C. The background signal (solid gray line) was obtained prior to the Se heat treatments. Selenization at 337 °C resulted in a considerable increase of Se signal at the CZTS/Mo interface, and a minor increase in the region between 100 and 800 nm from the surface, hereafter called “bulk”. The Se content close to the surface is about 2.5 times higher than that in the

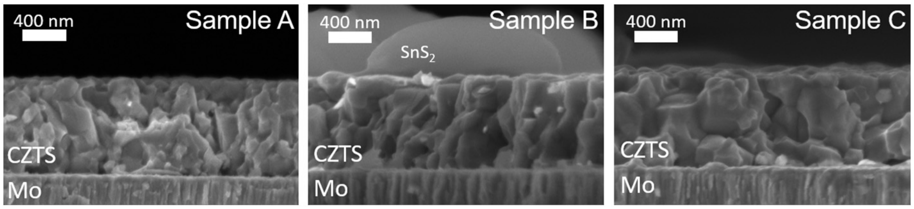

Fig. 2. Cross-sectional scanning electron microscopy (SEM) images of the CZTS samples A, B and C which was sulfurized at 500 °C for 10, 20 and 40 min respectively from the same precursor. Some SnS_2 is observed on the SEM image of sample B but was also seen on top of all samples with an optical microscope.